Available online at www.sciencedirect.com
ScienceDirect
Advances in Water Resources 30 (2007) 1046–1052
Advances in Water Resources
www.elsevier.com/locate/advwatres

Modelling tidal signals enhanced by a submarine spring in a coastal confined aquifer extending under the sea

Hailong Li [a,b,*], Ling Li [c,d], David Lockington [c], Michel C. Boufadel [e], Guanyi Li [a]

[a] *Department of Mathematics, Anshan Normal University, Anshan 114005, PR China*
[b] *School of Environmental Studies & (MOE) Biogeology and Environmental Geology Lab, China University of Geosciences, Wuhan 430074, PR China*
[c] *Environmental Engineering Division, School of Engineering, The University of Queensland, Brisbane 4072, Australia*
[d] *Centre for Eco-Environmental Modelling, State Key Laboratory of Hydrology-Water Resources and Hydraulic Engineering, Hohai University, Nanjing 210098, PR China*
[e] *Department of Civil and Environmental Engineering, Temple University, 1947 N. 12th Street, Philadelphia, PA 19122, USA*

Received 22 June 2006; received in revised form 28 September 2006; accepted 29 September 2006
Available online 22 November 2006

Abstract

Submarine springs discharge offshore groundwater from confined aquifers extending under the sea. The effects of these springs on the propagation of tidal oscillations in coastal confined aquifers are not known. This paper presents an approximate analytical solution of tidal head fluctuations in a confined aquifer with one submarine spring. The aquifer is assumed to extend in all directions infinitely. The spring is represented by a permeable round column on the seabed, which penetrates completely the impermeable layer overlying the confined aquifer. The error of the approximate solution is negligible if the distance from the spring to the coastline is much greater than the radius of the permeable column representing the spring. Through a hypothetical example, we demonstrate that it is possible to identify the spring's location using tidal signals observed from inland wells. Tidal groundwater head fluctuations from three inland observation wells at least are needed to determine the 5 model parameters, including the location (2 parameters), the radius of the permeable column representing the spring, the diffusivity of the aquifer, and the tidal loading efficiency of the system.

Keywords: Submarine groundwater discharge; Submarine springs; Coastal aquifer; Tide; Tidal wave propagation in aquifer; Tidal loading efficiency

1. Introduction

Submarine springs represent an important freshwater resource offshore. They can carry fresh groundwater through confined aquifers up to 60 km out to sea [13]. Fishermen have known about these submarine springs for decades but kept their locations a secret because of the amount of fish the springs attract. However, submarine springs (called "wonky holes") in the Great Barrier Reef of Australia have been found to affect once-pristine inshore reefs because of the acidic water discharge from lands cleared for crops [3]. Although similar submarine springs have also been found on the Atlantic continental shelf and other coastal areas, it is a difficult task to locate these springs in general [13].

In this paper, we hypothesize that tidal signals in coastal confined aquifers are mediated by submarine springs and hence provide a means of locating them. Tide-induced head fluctuations in coastal confined aquifers extending under the sea have been modelled and analysed by a series of previous studies. Van der Kamp [15] considered a single coastal confined aquifer which extends under the sea infinitely. Li and Chen [6] studied the situation where the overlying layer of the aquifer extends under the sea for a finite distance. Both studies assumed that there is no leakage

* Corresponding author. Address: Department of Civil and Environmental Engineering, Temple University, 1947 N. 12th Street, Philadelphia, PA 19122, USA. Tel.: +1 215 204 8428; fax: +1 215 204 4696.

E-mail addresses: hailong@temple.edu (H. Li), l.li@uq.edu.au (L. Li), d.lockington@uq.edu.au (D. Lockington), boufadel@temple.edu (M.C. Boufadel), liguani@gmail.com (G. Li).

0309-1708/$ - see front matter
doi:10.1016/j.advwatres.2006.09.004

through the overlying confining layer. Li and Jiao [8] extended their work by taking into account the leakage of the confining unit. Liu [11] and Maas and De Lange [12] examined the tidal signals observed in inland confined aquifers under tidal rivers.

So far, to the authors' knowledge, there is no report of studies in the literature on modelling the effect of a submarine spring on the propagation of tidal waves in a coastal confined aquifer extending under the sea. Here, we present a mathematical model for assessing such an effect. The aquifer is assumed to extend both seaward and landward infinitely, and to be overlain by an impermeable layer. The submarine spring is represented by a highly permeable round column on the seabed, which penetrates completely the impermeable layer. An approximate analytical solution to the model is derived with maximum errors quantified and shown to be negligible under realistic conditions. Using a hypothetical example, we demonstrate how the analytical solution can be applied together with data of observed tidal groundwater fluctuations in inland wells to estimate the location of the spring and other relevant model parameters such as the radius of the permeable column representing the spring, the diffusivity of the aquifer, and the tidal loading efficiency.

2. Mathematical model and analytical solution

2.1. Model setup

We consider a submarine confined aquifer with a spring represented by a highly permeable round column penetrating completely the overlying impermeable layer of the aquifer (Fig. 1). The round column is assumed so permeable that the seawater is directly connected to the confined aquifer in the column. Both the aquifer and its overlying impermeable layer extend in all directions infinitely, and are horizontal, homogeneous and with constant thickness. The bottom of the confined aquifer is impermeable. The coastline is assumed to be straight. An x–y Cartesian coordinates system is used with the y-axis chosen in the alongshore direction and the x-axis being positive seaward and extending through the centre of the spring hole (see Fig. 1). Based on the above assumptions and definitions, the following governing equations can be used to describe the head fluctuations within the confined aquifer [15]:

In the offshore aquifer ($x > 0$)

$$\frac{\partial h}{\partial t} = D\left(\frac{\partial^2 h}{\partial x^2} + \frac{\partial^2 h}{\partial y^2}\right) + L_e \frac{\mathrm{d}h_s}{\mathrm{d}t}, \quad x > 0,$$
$$(x - x_0)^2 + y^2 > R^2, \quad -\infty < t < +\infty. \tag{1}$$

In the inland aquifer ($x < 0$)

$$\frac{\partial h}{\partial t} = D\left(\frac{\partial^2 h}{\partial x^2} + \frac{\partial^2 h}{\partial y^2}\right), \quad x < 0, \ -\infty < t < +\infty. \tag{2}$$

$h(x, y, t)$ and D are the hydraulic head [L] and diffusivity [L^2T^{-1}] of the confined aquifer, respectively (the diffusivity is defined as the ratio of the storativity (dimensionless) to the transmissivity [L^2T^{-1}] of the confined aquifer); t is time [T] (here only the periodic solution is considered, i.e., no initial time); x_0 is the distance [L] between the centre of the spring hole and the coastline; R is the equivalent radius [L] of the spring (radius of the round, highly permeable column representing the spring); L_e is the loading efficiency (dimensionless) of the sea tide [16]; and $h_s(t)$ is the hydraulic head of the sea tide [L]. Given the linearity of the model, we consider only one tidal constituent as given by

$$h_s(t) = A\cos(\omega t), \tag{3a}$$

where A is the amplitude [L] of the tidal fluctuation and ω is the frequency [Rad T^{-1}] defined as

$$\omega = 2\pi/t_0, \tag{3b}$$

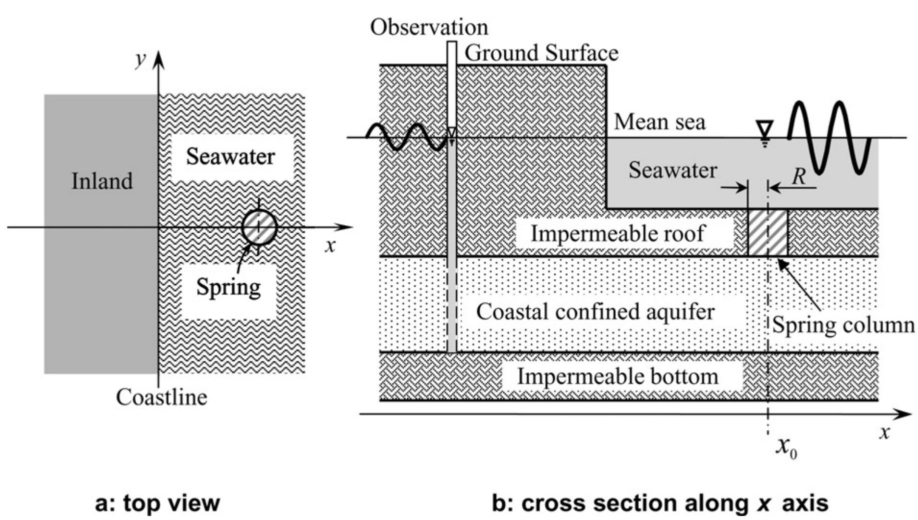

Fig. 1. An idealized confined aquifer extending under the sea with a permeable column representing a submarine spring.

in which t_0 is the tidal period [T]. Here the datum is set to be the mean sea level.

Since our focus is on the tidal signals as enhanced by the spring, the other forcing on the aquifer, such as the recharge, is ignored; so no-flow boundary conditions are applied at places sufficiently far from the spring, i.e.,

$$\lim_{x\to\pm\infty}\frac{\partial h}{\partial x}=\lim_{y\to\pm\infty}\frac{\partial h}{\partial y}=0. \tag{4}$$

At the coastline ($x=0$), the continuity of the hydraulic head and flux yields, respectively,

$$\lim_{x\to 0^+} h=\lim_{x\to 0^-} h,\quad \text{and} \tag{5}$$

$$\lim_{x\to 0^+}\frac{\partial h}{\partial x}=\lim_{x\to 0^-}\frac{\partial h}{\partial x}. \tag{6}$$

It is assumed that the round column equivalently representing the spring is highly permeable and short in its vertical extent, and so the head loss inside the column can be neglected. That is to say, approximately the seawater is directly connected to the aquifer at the bottom of the column; therefore, along the perimeter of the column's bottom, the following Dirichlet boundary condition applies

$$h|_{(x,y)\in\Gamma}=h_s(t)=A\cos(\omega t), \tag{7}$$

where $\Gamma=\{(x,y)|(x-x_0)^2+y^2=R^2\}$ is the boundary of the column equivalently representing the spring. Here it is further assumed that the density difference between the groundwater and the seawater can be neglected due to its minor effect on tidal groundwater head fluctuations [6].

2.2. Approximate analytical solution

An approximate analytical solution to the boundary-value problem (1)–(7) is derived (see Appendix A for details of the derivation). The approximate solution reads

$$h_{\text{approx}}(ax,ay,t;ax_0,aR,L_e)=h_1(ax,t;L_e)+h_2(ax,ay,t;ax_0,aR,L_e) \tag{8a}$$

with

$$h_1(ax,t;L_e)=\begin{cases}A\frac{L_e}{2}e^{ax}\cos(\omega t+ax), & x\leqslant 0,\\ AL_e\left[\cos(\omega t)-\frac{1}{2}e^{-ax}\cos(\omega t-ax)\right] & x>0,\end{cases} \tag{8b}$$

and

$$h_2(ax,ay,t;ax_0,aR,L_e)=A\,\text{Re}\left\{\left[1-L_e+\frac{L_e}{2}e^{-ax_0(1+i)}\right]\frac{K_0[ar(1+i)]e^{i\omega t}}{K_0[aR(1+i)]}\right\},\quad r\geqslant R, \tag{8c}$$

where

$$a=\sqrt{\frac{\omega}{2D}} \tag{8d}$$

is the confined aquifer's tidal propagation parameter or wave number [L^{-1}]; Re denotes the real part of the followed complex expression; $i=\sqrt{-1}$; K_0 is the modified Bessel function of the second kind and zeroth order [2]; $r=\sqrt{(x-x_0)^2+y^2}$ is the radius from point (x,y) to the centre of the spring hole $(x_0,0)$.

3. Discussion and application of the solution

3.1. Error analysis of the approximate solution

The maximum error between the approximate solution (8a) and exact solution to Eqs. (1)–(7) occurs on the boundary $\Gamma=\{(x,y)|(x-x_0)^2+y^2=R^2\}$ of the column representing the spring and equals (see Appendix A for its derivation)

$$E_{\max}(ax_0,aR)=\frac{AL_e e^{-ax_0}}{2}\sqrt{e^{2aR}+1-2e^{aR}\cos(aR)}. \tag{9}$$

The value ranges of a, R and x_0 may be assumed to be 10^{-5}–10^{-2} m^{-1} [9], 1–10^2 m and 10^2–10^4 m, respectively. So the value ranges of aR and ax_0 are $10^{-5}\leqslant aR\leqslant 1$ and $10^{-3}\leqslant ax_0\leqslant 100$. It is reasonable to assume $x_0\gg R$. Fig. 2 shows how the relative maximum error $E_{\max}(ax_0, aR)/(AL_e)$ changes with aR for $x_0=5R$, $10R$ and $20R$, respectively. One can see that the relative error is less than 6% for all the cases considered and less than 1.5% when $x_0\geqslant 20R$. In addition, these maximum errors occur on the boundary of the column representing the spring, and the error of the solution decreases as $r=\sqrt{(x-x_0)^2+y^2}$ increases. Therefore, the solution (8) has adequate accuracy in approximating the exact solution to (1)–(7) if $x_0\gg R$ and $r\gg R$.

3.2. Basic properties of the approximate solution

If there is no spring, i.e., $R\to 0^+$ in Eq. (8a), one can show

$$\lim_{R\to 0^+} h_{\text{approx}}(ax,ay,t;ax_0,aR,L_e)=h_1(ax,t;L_e), \tag{10}$$

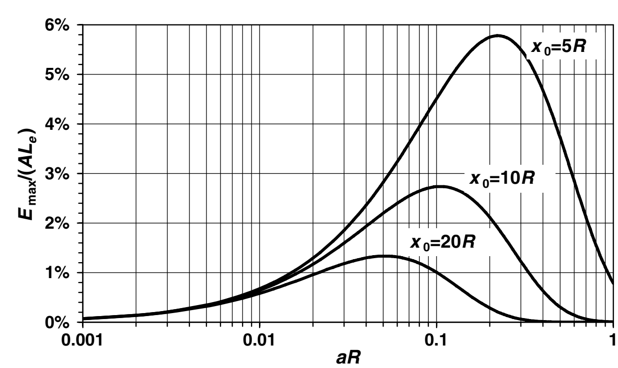

Fig. 2. Change of the maximum relative error $E_{\max}(ax_0,aR)/(AL_e)$ with dimensionless equivalent radius aR of the spring for different values of x_0/R.

where $\lim_{R\to 0^+}|K_0(aR)| = \infty$ has been applied. Eq. (10) indicates that $h_1(ax, t; L_e)$ describes the groundwater head fluctuation of the confined aquifer caused by only the tidal loading above the offshore part of the aquifer without spring. The solution $h_1(ax, t; L_e)$ is essentially the same as that by Ver der Kamp [15] where the confined aquifer extends under the sea infinitely.

From Eqs. (8a)–(8d), it can be seen that four independent parameters are involved in the model: the tidal loading efficiency L_e, the confined aquifer's tidal propagation parameter a, the equivalent radius R of the spring and the distance from the spring's centre to the coastline x_0. Given the simplicity of the expressions of $h_1(ax, t; L_e)$ and the coefficient $1 - L_e + \frac{L_e}{2}e^{-ax_0(1+i)}$ in Eq. (8c), only the dependence of the tidal head fluctuation on the dimensionless equivalent radius aR of the spring will be discussed here. The function $K_0[aR(1+i)]$ has the following properties: $\lim_{R\to 0^+}|K_0[aR(1+i)]| = \infty$, and its magnitude and argument ($|K_0[aR(1+i)]|$ and $\arg\{K_0[aR(1+i)]\}$) decrease as aR increases. Therefore, the amplitude and argument of the fluctuation, as given by Eq. (8c), increase with the spring's equivalent radius.

3.3. Hypothetical application example: locating the submarine spring using tidal data

The example is designed to demonstrate how the location of the spring can be determined using the approximate analytical solution (8) and observed tidal data in inland boreholes. The solution is first used to generate the "observed" data with the following values of model parameters: $x_0 = 1$ km, $R = 50$ m, $L_e = 0.5$, $A = 1.0$ m, $t_0 = 12.42$ h and $a = 0.0003\ \mathrm{m}^{-1}$. Hourly time series of fluctuating groundwater heads are generated for 51 hours (slightly more than 4 tidal cycles) at three observation wells: (x_k, y_k) $(k = 1, 2, 3)$ with $x_1 = -0.4$ km, $x_2 = x_3 = -0.1$ km, $y_1 = 3$ km, $y_2 = 1.2$ km and $y_3 = -0.3$ km (see Fig. 3). These head data are then perturbed by random numbers ranging between −0.01 m and 0.01 m to represent the observation errors. Fig. 4 shows the tidal level fluctuation and the "observed" head data in the three wells.

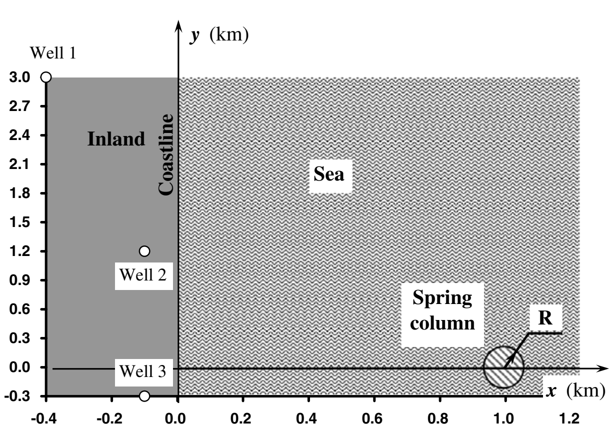

Fig. 3. Locations of the spring and three inland observation wells.

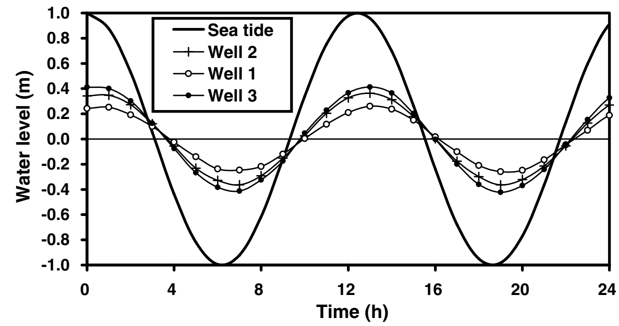

Fig. 4. Oscillations of sea level with time and the generated hourly data of groundwater heads in the three observation wells.

We then formulate the inverse problem by assuming that the values of the five model parameters (L_e, a, ax_0, aR and ay_3) are unknown and may be estimated based on the "observed" groundwater head data at the three wells. Note that the relative locations of the three wells (i.e., x_k $(k = 1, 2, 3)$ and $y_k - y_3$ $(k = 1, 2)$) are known. By comparing the "estimated" and the "true" values of the five parameters, the applicability and reliability of the tidal method in locating the spring are examined and demonstrated. For the system considered here ($L_e = 0.5$, $ax_0 = 20aR$ and $aR = 0.015$), the result in Fig. 2 indicates that the error of the approximate solution (8) is less than 0.5% of the tidal amplitude. So the approximate solution can be used without much loss of accuracy.

Based on the solution (8), the five parameters are estimated by solving the following least-squares problem:

$$\min_{\log a, ay_3, \mathbf{P}} \sum_{j=1}^{51} \sum_{k=1}^{3} [h_{\text{approx}}(10^{\log a}x_k, 10^{\log a}(y_k - y_3) + ay_3, t_j; \mathbf{P}) - h^*_{kj}]^2, \tag{11}$$

where $\mathbf{P} = (L_e, ax_0, \log(aR))$ is the parameter vector; $h_{\text{approx}}(10^{\log a}x_k, 10^{\log a}(y_k - y_3) + ay_3, t_j; \mathbf{P}) \equiv h_{\text{approx}}(ax_k, ay_k, t_j; \mathbf{P})$ is the solution given by (8) at the kth observation well $(x_k, y_k)(k = 1, 2, 3)$ for time t_j where $t_j = j - 1$ (h) is the jth observation time; h^*_{kj} $(j = 1, \ldots, 51;\ k = 1, 2, 3)$ are the 51 hourly "observed" groundwater head data at the kth observation well (x_k, y_k) $(k = 1, 2, 3)$. Here, the logarithmic transformations of a and aR are used instead of the parameters themselves because, for nonlinear least-squares inverse problems, these transformations can speed up the convergent speed of the iteration and avoid the computation of negative parameter values in the iteration (e.g., [1,7,10]).

A Fortran code was developed to solve numerically the least-squares problem, where the Bessel function is calculated by their definition series (see, e.g., Appendix III of Carslaw and Jaeger [2]). The estimated parameter values are listed in Table 1. More than a dozen of different initial guess values of the parameters were used and their ranges are also listed in Table 1. All these initial guess values converged to the same result. One can see from Table 1 that

Table 1
Ranges of initial guess values, true and estimated values of the five model parameters for the hypothetical example

	$\log(a)$	ay_3	L_e	ax_0	$\log(aR)$	a	aR	x_0	R	y_3
Initial value ranges	$[-4, -2]$	$[-1, 0.4]$	[0, 1]	[0.1, 1]	$[-3, -1]$					
True values	−3.52	−0.090	0.500	0.300	−1.824	3.0×10^{-4}	0.015	1000	50	−300
Estimated values	−3.52	−0.0801	0.505	0.305	−1.818	3.01×10^{-4}	0.0152	1014	50.5	−266
Relative error (%)[a]	0.04	11.05	0.97	1.67	0.31	0.31	1.30	1.36	0.99	11.32

[a] The relative error is defined as the absolute value of the ratio of the difference between the true and estimated value to the true value.

the estimated parameter values are very close to their respective "true values". The relative errors of all the estimated parameters other than ay_3 and y_3 are less than 2%. These errors are likely to have been caused by the "observation" errors ranging between −0.01 m and 0.01 m.

Theoretically, for the single-component oceanic tide, the data of each observation well can provide 2 equations for fitting the amplitude and phase of the sinusoidal head fluctuation. Therefore, three wells can provide 6 equations which may be independent of each other. The foregoing example indicates that the 6 equations provided by the three given wells can uniquely determine the five independent parameters including the location (two parameters) and equivalent radius of the spring, the tidal loading efficiency and the diffusivity of the confined aquifer. Numerical tests also indicate that the minimum well number to uniquely determine the 5 parameters is 3. For example, if the second well was not included, the iteration to minimize (11) either converged to different values for different initial guesses or even failed to converge.

If the oceanic tide comprises both semidiurnal and diurnal components, as is commonplace in reality, then the number of equations provided by each well is doubled because the amplitudes and phase shifts of both components can be fitted. In this case one may intuitively think that the well number required to uniquely determine the 5 model parameters may be reduced. Unfortunately, our numerical tests using two-component oceanic tides indicated that this is not the case: if the second well was not included, the model parameters in (11) either converged to different values for different initial guesses or even did not converge at all. This suggests that the equations of the diurnal and semidiurnal components for amplitude and phase are not independent. It is common among various analytical solutions of tidal groundwater head fluctuations that the equations for amplitude and phase are not independent for different tidal components or even different spatial locations, for example, the analytical solution by Jacob [5].

To examine the effect of well locations on determining the model parameters, the y-coordinate of the third well was changed from −300 m to 300 m so that all three wells are located on the same side of the x-axis and the inverse problem was solved with the other conditions unchanged. The estimated parameter values were also found to be very close to their respective "true values". The relative errors of all the estimated parameters other than ay_3 and y_3 are less than 2%. A problem encountered in this case is that, for some initial guesses of parameter values, the minimizing process converged to local minimums that were significantly greater than the global minimum. Our further numerical tests showed that increasing the amount of observation data by either collecting more data (longer time series) from the exiting wells or adding new well(s) improves the accuracy of parameter estimates and convergence of the minimization process to the global minimum.

4. Concluding remarks

We have derived an approximate analytical solution to describe the groundwater head fluctuations in a coastal confined aquifer induced by both the tidal loading on the aquifer's offshore roof and transmission of tidal pressure oscillations through a submarine spring. The error analysis shows that the accuracy of the solution is acceptable if the distance from the spring to the coastline is much greater than the equivalent radius of the spring, a condition that is likely to hold in reality.

Through a hypothetical example, we have demonstrated how this analytical solution can be used together with data of observed tidal groundwater fluctuations in inland wells to estimate the location of the submarine spring. Numerical tests show that at least three inland observation wells are needed in order to determine the spring's location (two parameters) and other three parameters involved in the system. The discovery of submarine springs has been so far accidental and extremely difficult. The method proposed here may provide guidance for future search for these ecologically important point sources of freshwater in offshore marine environment.

Acknowledgements

Part of this work was done when the first author visited Division of Environmental Engineering, School of Engineering, The University of Queensland, Australia. The research was supported by the National Natural Science Foundation of China (No. 40372111) and the Australian Research Council Discovery grants (No. DP0346461).

Appendix A. Derivation of the approximate solution (8) and the error estimation (9)

Direct inspection indicates that $h_1(ax, t; L_e)$ satisfies the following equations:

$$\frac{\partial h_1}{\partial t} = D\left(\frac{\partial^2 h_1}{\partial x^2} + \frac{\partial^2 h_1}{\partial y^2}\right) + L_e \frac{\mathrm{d}h_s}{\mathrm{d}t}, \quad x > 0, \ -\infty < t < +\infty, \tag{A.1}$$

$$\frac{\partial h_1}{\partial t} = D\left(\frac{\partial^2 h_1}{\partial x^2} + \frac{\partial^2 h_1}{\partial y^2}\right), \quad x < 0, \ -\infty < t < +\infty, \tag{A.2}$$

$$\lim_{x\to\pm\infty} \frac{\partial h_1}{\partial x} = \lim_{y\to\pm\infty} \frac{\partial h_1}{\partial y} = 0, \tag{A.3}$$

$$\lim_{x\to 0^+} h_1 = \lim_{x\to 0^-} h_1, \quad \text{and} \tag{A.4}$$

$$\lim_{x\to 0^+} \frac{\partial h_1}{\partial x} = \lim_{x\to 0^-} \frac{\partial h_1}{\partial x}. \tag{A.5}$$

Let

$$h_{2\mathrm{Exact}} = h - h_1. \tag{A.6}$$

Given the linearity of the model (1)–(6) one can show from Eqs. (1)–(7) and (A.1)–(A.5) that $h_{2\mathrm{Exact}}$ satisfies the following equations:

$$\frac{\partial h_{2\mathrm{Exact}}}{\partial t} = D\left(\frac{\partial^2 h_{2\mathrm{Exact}}}{\partial x^2} + \frac{\partial^2 h_{2\mathrm{Exact}}}{\partial y^2}\right),$$
$$(x-x_0)^2 + y^2 > R^2, \ -\infty < t < +\infty, \tag{A.7}$$

$$h_{2\mathrm{Exact}}|_{(x,y)\in\Gamma} = A(1-L_e)\cos(\omega t) + A\frac{L_e}{2}\mathrm{e}^{-ax}\cos(\omega t - ax),$$
$$(x-x_0)^2 + y^2 = R^2, \tag{A.8}$$

$$\lim_{x\to\pm\infty} \frac{\partial h_{2\mathrm{Exact}}}{\partial x} = \lim_{y\to\pm\infty} \frac{\partial h_{2\mathrm{Exact}}}{\partial y} = 0. \tag{A.9}$$

Due to the complexity of the boundary condition (A.8), it is extremely difficult if not impossible to find the exact analytical solution $h_{2\mathrm{Exact}}$. Here we search for an approximate analytical solution instead. Replacing $\mathrm{e}^{-ax}\cos(\omega t - ax)$ in (A.8) with $\mathrm{e}^{-ax_0}\cos(\omega t - ax_0)$ leads to the following simplified, spatially constant boundary condition:

$$h_{2\mathrm{Exact}}|_{(x,y)\in\Gamma} \approx h_2|_{(x,y)\in\Gamma}$$
$$\stackrel{\text{def.}}{=} A\,\mathrm{Re}\left\{(1-L_e)\exp(\mathrm{i}\omega t) + \frac{L_e}{2}\exp[-ax_0 + \mathrm{i}(\omega t - ax_0)]\right\}. \tag{A.10}$$

Note that the solution of (A.7), (A.9) and (A.10) is axisymmetric with respect to the centre of the spring hole. Using the polar coordinates (r, θ) with the origin at the centre of the spring, we introduce $H_2(r,t)$ as a complex function of the real variables $r = \sqrt{(x-x_0)^2 + y^2}$ and t; this function satisfies Eqs. (A.7), (A.9) and (A.10) with the right-hand side of (A.10) replaced by $A\{(1-L_e)\exp(\mathrm{i}\omega t) + \frac{L_e}{2}\exp[-ax_0 + \mathrm{i}(\omega t - ax_0)]\}$. Let h_2 be the real part of the solution to (A.7), (A.9) and (A.10), i.e.,

$$h_2 = \mathrm{Re}[H_2(r,t)]. \tag{A.11}$$

Now suppose

$$H_2(r,t) = AZ(r)\exp(\mathrm{i}\omega t), \tag{A.12}$$

where $Z(r)$ is an unknown function of r. Substituting (A.12) into (A.7), (A.9) and (A.10) and then dividing the results by $A\exp(\mathrm{i}\omega t)$ yield

$$\mathrm{i}\omega Z = D\left(\frac{\partial^2 Z}{\partial r^2} + \frac{1}{r}\frac{\partial Z}{\partial r}\right), \quad r = \sqrt{(x-x_0)^2 + y^2} > R, \tag{A.13}$$

$$\lim_{r\to\infty} \frac{\partial Z}{\partial r} = 0, \tag{A.14}$$

$$Z(r)|_{r=R} = (1-L_e) + \frac{L_e}{2}\exp[-ax_0(1+\mathrm{i})]. \tag{A.15}$$

Using a similar method to that in Hsieh and Bredehoeft [4] or Carslaw and Jaeger [2], one can obtain the solution to (A.13)–(A.15):

$$Z(r) = \left[1 - L_e + \frac{L_e}{2}\mathrm{e}^{-ax_0(1+\mathrm{i})}\right]\frac{K_0[ar(1+\mathrm{i})]}{K_0[aR(1+\mathrm{i})]}, \quad r \geqslant R, \tag{A.16}$$

where $K_0(z)$ is the modified Bessel function of the second kind and zeroth order. Finally, combining Eqs. (A.11), (A.12) and (A.16), we obtain the solution h_2 as given by (8c). Then using (A.6), we find

$$h = h_1 + h_{2\mathrm{Exact}} \approx h_1 + h_2 \stackrel{\text{def.}}{=} h_{\mathrm{approx}}, \tag{A.17}$$

which is the approximate solution given by (8a).

Now consider the error between the exact solution $h_{2\mathrm{Exact}}$ of (A.7)–(A.9) and its approximation h_2. Let

$$E = h_{2\mathrm{Exact}} - h_2. \tag{A.18}$$

According to (A.7)–(A.10), E satisfies the governing Eq. (A.7) and the boundary condition (A.9), and on the boundary of the column representing the spring, we have

$$E|_{(x,y)\in\Gamma} = A\frac{L_e}{2}[\mathrm{e}^{-ax}\cos(\omega t - ax) - \mathrm{e}^{-ax_0}\cos(\omega t - ax_0)],$$
$$(x-x_0)^2 + y^2 = R^2. \tag{A.19}$$

The maximum principle of the linear partial differential equations of parabolic type (e.g., [14], p232) indicates that the maximum and minimum of the error E only occur on the boundary of the column representing the spring. Thus,

$$\begin{aligned}
|E|_{\max} &\leqslant \max E|_{(x,y)\in\Gamma} = \max_{|x-x_0|\leqslant R} A\frac{L_e}{2}|\mathrm{e}^{-ax}\cos(\omega t - ax) \\
&\quad - \mathrm{e}^{-ax_0}\cos(\omega t - ax_0)| \\
&= \max_{|x-x_0|\leqslant R} \frac{AL_e}{2}|\mathrm{Re}[\mathrm{e}^{-ax(1+\mathrm{i})+\mathrm{i}\omega t} - \mathrm{e}^{-ax_0(1+\mathrm{i})+\mathrm{i}\omega t}]| \\
&\leqslant \max_{|x-x_0|\leqslant R} \frac{AL_e}{2}|\mathrm{e}^{-ax(1+\mathrm{i})+\mathrm{i}\omega t} - \mathrm{e}^{-ax_0(1+\mathrm{i})+\mathrm{i}\omega t}| \\
&= \frac{AL_e\mathrm{e}^{-ax_0}}{2}\max_{|x-x_0|\leqslant R}|\mathrm{e}^{a(x_0-x)(1+\mathrm{i})} - 1| \leqslant \frac{AL_e\mathrm{e}^{-ax_0}}{2}|\mathrm{e}^{aR(1+\mathrm{i})} - 1| \\
&= \frac{AL_e\mathrm{e}^{-ax_0}}{2}\sqrt{\mathrm{e}^{2aR} + 1 - 2\mathrm{e}^{aR}\cos(aR)} \stackrel{\text{def.}}{=} E_{\max}(ax_0, aR)
\end{aligned} \tag{A.20}$$

This gives the error estimation Eq. (9).

References

[1] Carrera J, Neuman SP. Estimation of aquifer parameters under transient and steady state conditions: 1 Maximum likelihood method incorporating prior information. Water Resour Res 1986;22:199–210.

[2] Carslaw HS, Jaeger JC. Conduction of heat in solids. 2nd ed. Clarendon Press; 1959.

[3] Gagan MK, Ayliffe LK, Opdyke BN, Hopley D, Scott-Gagan H, Cowley J. Coral oxygen isotope evidence for recent groundwater fluxes to the Australian Great Barrier Reef. Geophys Res Lett 2002;29(20):1982. doi:10.1029/2002GL015336.

[4] Hsieh PA, Bredehoeft JD. Determination of aquifer transmissivity from earth tide analysis. Water Resour Res 1987;23(10):1824–32.

[5] Jacob CE. Flow of groundwater. In: Rouse H, editor. Engineering hydraulics. New York: John Wiley; 1950. p. 321–86.

[6] Li G, Chen C. Determining the length of confined aquifer roof extending under the sea by the tidal method. J Hydrol 1991;123:97–104.

[7] Li HL, Yang QC. A least-squares penalty method algorithm for the inverse problems of steady state aquifer models. Adv Water Resour 2000;23(8):867–80.

[8] Li HL, Jiao JJ. Tide-induced groundwater fluctuation in a coastal leaky confined aquifer system extending under the sea. Water Resour Res 2001;37(5):1165–71.

[9] Li HL, Jiao JJ. Analytical studies of groundwater-head fluctuation in a coastal confined aquifer overlain by a leaky layer with storage. Adv Water Resour 2001;24(5):565–73.

[10] Li HL, Jiao JJ, Luk M. A falling-pressure method for measuring air permeability of asphalt in laboratory. J Hydrol 2004;286(1–4):69–77.

[11] Liu K. Tide-induced ground-water flow in deep confined aquifer. J Hydraul Eng 1996;122(2):104–10.

[12] Maas C, De Lange WJ. On the negative phase shift of groundwater tides near shallow tidal rivers – the Gouderak anomaly. J Hydrol 1987;92:333–49.

[13] Nowak R. 'Wonky holes' blamed for coral death, Exclusive from New Scientist Print Edition, Melbourne, 2002. <http://www.newscientist.com/article.ns?id=dn3049>.

[14] Ockendon J, Howison S, Lacey A, Movchan A. Applied partial differential equations. Oxford, New York: Oxford University Press; 1999.

[15] Van der Kamp G. Tidal fluctuations in a confined aquifer extending under the sea. In: Proceedings of 24th international geological congress, Section 11, 1972. p. 101–6.

[16] Van der Kamp G, Gale JE. Theory of earth tide and barometric effects in porous formations with compressible grains. Water Resour Res 1983;19(2):538–44.